Journal of Applied Polymer Science

Synthesis of Biocompatible and Degradable Microspheres Based on 2-Hydroxyethyl Methacrylate via Microfluidic Method

Mohammad Tarameshlou,[1] Seyed Hassan Jafari,[1] Iraj Rezaeian,[1] Hossein Ali Khonakdar[2]
[1]School of Chemical Engineering, University College of Engineering, University of Tehran, P.O. Box 11155-4563, Tehran, Iran
[2]Iran Polymer and Petrochemical Institute, P.O. Box 14965-115, Tehran, Iran
Correspondence to: S. H. Jafari (E-mail: shjafari@ut.ac.ir)

ABSTRACT: Monodisperse poly(2-hydroxyethyl methacrylate), p-HEMA, microspheres in size ranging from 16 to 340 (μm) were synthesized by *in situ* emulsion photopolymerization of HEMA monomer with polyethylene glycol diacrylate (p-EGDA) by means of a three-dimensional microfluidic flow-focusing device. An aqueous solution of HEMA, p-EGDA as chain extender and UV-photoinitiator serving as dispersed phase formed microdroplets in a continuous oil phase mainly consisting of n-heptane. A downward coaxial orifices design in the device led to confinement of the reaction admixtures thread to central axis of the microchannels. This design strategy could solve the wetting problem of dispersed phase with the microchannels leading to a successful production of monodisperse microspheres with size variation of less than 4%. The effects of concentration of p-EGDA, surfactant, and flow rate ratios on microsphere size were examined. It was observed that increasing the concentration of p-EGDA slightly increases the size whereas increasing the flow rate ratios of continuous to dispersed phase effectively decreases the size of microspheres. The rapid continuous synthesis of p-HEMA based microspheres via the microfluidic route with reliable control over size, size distribution, and composition opens new doors for mass production of biocompatible and degradable polymeric microspheres for enormous biotechnological applications. © 2014 Wiley Periodicals, Inc. J. Appl. Polym. Sci. **2014**, *131*, 40925.

KEYWORDS: biodegradable; microfluidics; morphology

Received 3 October 2013; accepted 27 April 2014
DOI: 10.1002/app.40925

INTRODUCTION

Interest in miniaturization of biological and medical systems has grown in recent years. The nano and/or micron size polymeric particles can be used as smart delivery systems, which can carry molecules and drugs to target sites directly. These particles can also be used as essential components for artificial cells, bioreactors, biosensors, chromatography, and information storage. Drugs, hormones, proteins, nucleic acid, peptides, and antibodies can be carried by micro and nanoparticles through various routes of administration.[1–3] Those applications primarily depend on particle size, shape, morphology, and size distribution.[4–6] It is worth to note that the useful size range for many biomaterial particles is in the range of several micrometers to few nanometers. For example, the ideal sizes for encapsulation or drug delivery systems are in the microns range.[7,8] Moreover, narrowing particle size distribution has been shown to be important in controlling drug release kinetics, reproducibility, and bioavailability[9] (different size particles are accumulated differently in the body).

In general, biocompatible and biodegradable polymeric microparticles have become strong candidates for encapsulating and using in drug delivery because of their ease of delivery, mechanical stability, mild processing conditions, high drug encapsulation efficiency, long-term sustained release, slow degradability, and the ability to regulate their drug release kinetics.[10] In recent years, the demand for hydrophilic media has rapidly increased with the development of biotechnology. Porous poly(2-hydroxyethyl methacrylate) (p-HEMA) microspheres are excellent media for applications in chromatographic separation, immobilization of bioactive molecules, designing bioreactor and biosensor, and drug delivery systems.[11] The p-HEMA has abundant hydroxyl groups on its surface which can be modified into different functional groups to meet the requirement for different chromatographic applications such as exchange chromatography, hydrophobic interaction chromatography, as well as affinity chromatography.[12] Moreover, the p-HEMA has excellent biocompatibility because of its hydrophilic functional groups, and therefore can be used in immobilization of bioactive molecules.[13]

Recently, innovative developments of microfluidic systems based on micro-electro-mechanical systems (MEMS) technologies have attracted great scientific and industrial attentions. A wide variety of chemical and physical phenomena occur in a designed microfluidic systems, which is fundamentally an area of research drawn from classical physics to chemistry-fluid mechanics, such

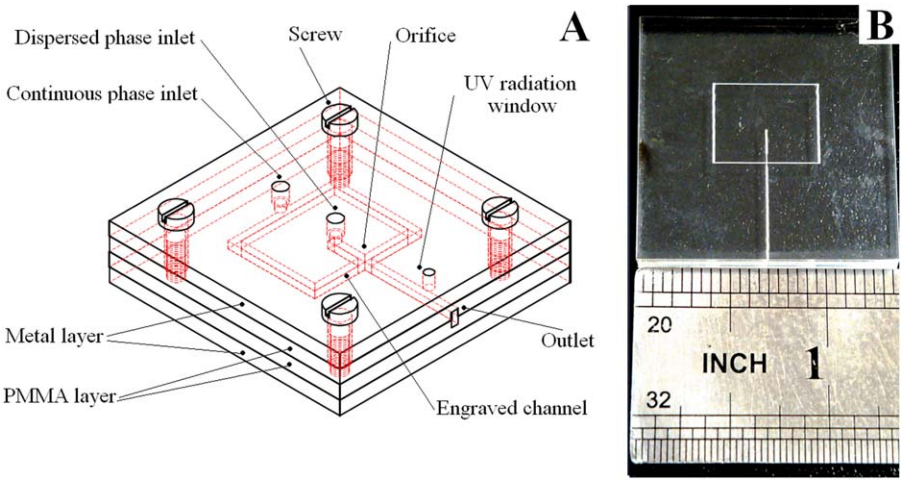

Figure 1. (A) Microfluidic device set up and constructed layers and (B) a typical photo of the engraved microchannels on bottom layer (PMMA sheet) by laser. [Color figure can be viewed in the online issue, which is available at wileyonlinelibrary.com.]

as electrostatics, thermodynamics, and statistical mechanics, elasticity, and polymer chemistry. In microfluidic systems, fluids flow in microchannels by diffusion-based laminar flow mechanism due to low Reynolds numbers. The rapid mass and heat exchanges in microchannels result in a higher throughput and a faster reaction process as compared to conventional systems.[14]

Recently, the microfluidic-based generation of microparticles has been extensively explored as an alternative versatile route for production of microdroplets based on emulsion mechanism.[15–18] Microfluidic platforms are shown to be useful in generation of monodisperse microdroplet emulsion by predictable breakup of immiscible coflowing streams forming discrete droplets with consistent size in a variety of microfluidic geometries.[19] In contrast to bulk emulsification methods, an emulsion in a microfluidic device is made by precisely fabricating one drop at a time which results in a highly monodisperse emulsion.[20] Moreover, if the generated microdroplets are polymerizable, it is possible to obtain thousands of polymer particles with well-defined characteristics such as size, shape, and morphology. With microfluidics it is also possible to form multiphase droplets from which partial polymer spheres, Janus, ternary polymer particles, polymeric beads, disks, and plugs can be fabricated.[21]

Moreover, efficient components and control of chemical reactions at microliter to deciliter scales allow microfluidic devices to introduce better control on synthesis and shape parameters. In these methods, the microbubble or microdroplet size, size distribution, flow behavior, and flow pattern need to be controlled, tuned, and manipulated in a precise way.[22,23] According to the type of flow in microchannels, the particle formation and synthesis methods can be primarily divided into two main categories: that is, single phase continuous flow synthesis and emulsion (two-phase) micro-droplets/segmented flow synthesis. In both categories; reaction times, temperatures, mixing efficiency, reactants and surfactant concentrations, contact conditions, viscosity, surface tension, and flow rates are parameters which control particle quality.[24]

Another attractive unique feature of the microfluidic platforms is ability to fabricate double, triple, and even higher order emulsions, where the size and number of the ordered and encapsulated droplets can be easily manipulated in a precise manner. Moreover, solid particles with controlled nonspherical shapes can be fabricated in two steps; first generating uniform droplets of the desired shape in a microfluidic platform and then solidifying the content of the droplet. As the morphology of droplets is determined only by the physical properties of the fluids and operating conditions (device geometry and flow rates), this method is a general way of synthesizing spherical particles of a variety of materials with dimensions in micrometer scale. By increasing the flow rate or surface tension of the dispersed phase, the volume of the droplet increases, and hence the shape of droplet changes from spheres into nonspherical shapes. The prepared droplets can then be solidified by light or by UV photo-induced polymerization, thermally induced polymerization, or through a liquid–solid phase transition at downstream.[24,25]

The aim of this research is to use a microfluidic device to synthesize monodisperse biocompatible and biodegradable microparticles based on p-HEMA. The strategies consist of microdroplet formation by a water-in-oil (W/O) emulsion mechanism in a cross-junction flow-focusing microfluidic channel, pre-*in situ* UV photopolymerization of microdroplet after the junction and consequently post UV curing of the prepared microparticles in a sedimentation tank to consolidate the microparticles. The effects of composition of the dispersed phase, and surfactants as well as the flow rate ratios on microparticle formation are discussed here.

EXPERIMENTAL

Materials and Methods

Materials. 2-Hydroxyethyl methacrylate (HEMA) as monomer and the main constituent of the dispersed phase, n-heptane as continuous phase, hexadecanoic acid (Palmitic acid) as surfactant, and 2-propanol were obtained from Merck (Germany). Other constituents, polyethylene glycol diacrylate (p-EGDA $M_n = 575$ g mol^{-1}) and 2-hydroxy-4′-(2-hydroxyethoxy)-2-methylpropiophenone (IRGACURE® 2959) as UV initiator were

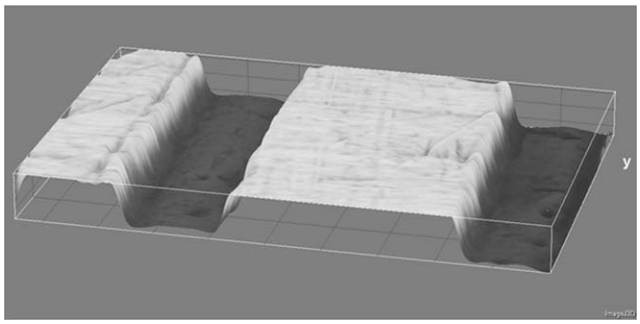

Figure 2. Surface profile/roughness of a typical microchannel obtained by ImageJ software.

purchased from Sigma–Aldrich (Germany). Filter papers, Cat No. 1442, were obtained from Whatman, Germany. A conventional poly(methylmethacrylate), (PMMA), extruded sheet (Ray Chung Acrylic Enterprise, China) was purchased from local market.

Fabrication of Microfluidic Device. The proposed 3D flow-focusing microfluidic device (3D-MFFD), 90° cross-junctions, was designed by AutoCAD® and constructed on two PMMA substrates with a CO_2 laser micromachining process (Guangdong Hans's Yueming Laser Tech, CMA-960, Taiwan). The microfluidic device had four layers namely (from top to bottom) a metal cover layer, upper channel layer, lower channel layer, and bottom metal layer [Figure 1(A)] which were fixed together by screw binding. A round observation area with diameter of 2 mm was designed at the channel width, after the cross-junction on downstream, as UV irradiation window for *in situ* photopolymerization. The screw binding and microfluidic chip fabrication process are low cost, easy to clean, and cheap to recycle.

To prepare channels in the required dimensions, a PMMA sheet was used to find appropriate beam power and motion speed to engrave channels of almost 150 and 250 (μm), while the layout comprises several straight channels with varying engraving parameters. Finally, the channels fabricated using a constant laser firing power 4 W and motion velocity of 2.5. A typical sample of the engraved microchannels on the PMMA sheet is shown in Figure 1(B). Afterwards, engraved sheets were cut and then sonicated (SONOREX SUPER RK-106, Germany) in 2-propanol for 5 min, rinsed with deionized water, and then dried in an oven at 30°C for 12 h. Flow connections and simple injection syringe were bound by cyano-acrylate adhesives and microfluidic chip layers were then tightened by screws.

As during microfluidic operation the flow rate of the feed depends on surface texture of the micro channels which certainly influence process and quality of microspheres, the surface profile/roughness of the microchannel is an important consideration. For this purpose, the surface profile/roughness of a typical microchannel was investigated by ImageJ software and the resulting image is presented in Figure 2. Based on this processed image, it is seen that there are no significant defects (roughness or harsh surface) on the surface of the microchannels to influence the fluid streams and procedure of microdroplets generation.

Table I. Some Characteristics of the Used Materials[a]

Materials	Density (g cm^{-3})	Viscosity (cP)	Solubility parameter (cal cm^{-3})$^{0.5}$
HEMA	1.07	5.9	23
p-EGDA	1.12	57	29.9
n-Heptane	0.679	0.42	7.5
p-HEMA	1.15	-	25-26

[a] The density and viscosity are reported by the manufacturer.

A UV lamp (18W OSRAM DULUX S-BLUE UVA, Germany) with light irradiation at 280–315 (nm) was used as the source of *in situ* photo-initiation. To initiate the *in situ* photopolymerization of formed microdroplets, the light was focused by a glass magnifier objective lens on the observation window in the upper metal layer of the device. Moreover, an extra UV lamp (9W OSRAM DULUX S-BLUE UVA, Germany) was used as post UV photopolymerization source on a 25 × 2 (cm × cm) aluminum tank where the semisolid microparticles sediment and stay to completely solidify by further polymerization. A cooling fan (Cooler Master Hyper XT3, Taiwan) was used on the back of the microfluidic device, that is, the bottom metal layer, for preventing the heat buildup in the channels during the UV irradiation.

To inject fluids, 1702RN (25 μL) syringe series (Hamilton), 0.5 (mL) insulin glass syringes were used to supply dispersed phase and also 1, 2.5, and 5 (mL) glass syringes with Teflon tubing were used to supply the continuous phase into the 3D-MFFD channels. Flow rates were controlled using two independent homemade syringe pumps to provide different flow rates.

Generation of Microdroplets in the Microfluidic Device

As shown in Figure 1(B), the microfluidic device fabricated with PMMA sheets consists of two inlets of continuous fluids with hydrophobic n-heptane solution and one inlet of hydrophilic solution as a dispersed phase. The dispersed phase and n-heptane solutions are immiscible because of their distinctive properties being hydrophilic and hydrophobic, respectively; therefore, they can easily form water-in-oil (W/O) emulsion in the microfluidic channel (Table I). The dispersed phase consisting of HEMA, chain extender, and photo-initiator was supplied from the central cross-junction shaped microchannel, and n-heptane with surfactant as continuous phase was injected perpendicularly from two side microchannels, where W/O emulsion was reproducibly formed by rupturing of hydrodynamic instability under the experimental condition [Figure 1(B)].

The formation of microdroplets at a junction is governed by the competition between the viscous stress and the surface tension stress.[26,27] The capillary number ($C_a = U\mu/\gamma$) is a value showing the relative importance of these two factors, where U is the flow rate of continuous phase, μ is the viscosity of the

continuous phase, and γ is the interfacial tension between the hydrophilic and continuous phases. The C_a can be modified by varying Q_c, the flow rate of the continuous phase, which results from a change in U through the relationship, $U = Q_c/A$, where A is the cross-sectional area of the microchannel. Therefore, calculation of C_a to depict stable and unstable emulsion microdroplet formation regimes and its dependency on the dispersed flow rate in the present 3D-MFFD is not applicable. The cross sectional area of the present cross channel could not be measured accurately due to the fact that the 3D-MFFD was prepared by the laser ablation process. It is more reliable to explore and depict regimes Q_d versus Q_c/Q_d ratio coordination instead of Q_d versus C_a. In this context, an optical measurement method and its decoding strategy were applied to explore stable and unstable regimes. To find the above-mentioned regimes for microdroplet formation, an electronic homemade device was designed which is introduced in the next section.

Finally, the flow patterns of the system in Q_c/Q_d and Q_d coordinates were depicted to investigate the condition for generation of monodisperse and stable microdroplets. No leakage was observed within the range of flow rates at which the process was tested. Moreover, the swelling of 3D-MFFD device caused by the dispersed phase and continuous phase solutions was not apparent during the experiments.

Synthesis of Microspheres

The process was performed by dispersed phase containing HEMA/p-EGDA in three different composition ratios (0, 4, and 8 wt % of p-EGDA) and UV photo-initiator (0.75 wt %). The flow rate of the dispersed phase was fixed at 0.4 (μL min^{-1}) while the continuous phase flow rates were varied from 3 to 10 (μL min^{-1}). The synthesis of microparticles was done in the stable regimes based on the explored flow patterns data. After changing the flow rates, the device was equilibrated for at least 1 min to ensure stable droplet formation and then UV exposure applied on the device for 1 min. The microfluidic device outlet was suspended in a rectangular tank containing at least 50 (mL) of continuous phase. The semipolymerized microparticles were left in this bath for at least 15 min while exposing to the second UV lamp to ensure complete post UV photopolymerization. The microparticles were separated by a filter paper and washed several times with pure n-heptane and then dried in an oven for 5 min at 30°C.

Analytical Instruments and Methods

To investigate microdroplet formation in stable and unstable forms, a homemade light intensity measurement device based on microcontroller was designed. The instrument consisted of a laser emitting diode, Patchcore optical fiber, and a photoreceiver sensor connected to microcontroller AVR-Atmel system [Figure 3(A)]. The design concept was based on light emitting to the surface of glass based microchannel, which was connected to downstream of the main 3D-MFFD, and measuring the light intensity at other side of the channel by a photoreceiver sensor. The collected intensity by the photoreceiver was translated to the changes in fluid turbidity based on differences between light transparency of the continuous phase and the semipolymerized microparticles while passing in front of the sensor. Shortly, the light intensity decreases when a semipolymerized microparticle crosses the sensor surface while continuous phase has no effect on the light intensity during the process. Therefore, each microparticle can be detected when light intensity decreases. Moreover, the sequence of light intensity fluctuation can be translated into the microparticle moving speed and/or size. In other words, instability of microparticle formation and either size deviation can be detected when there are no light intensity fluctuations. Typical examples of the microcontroller data, stable and unstable regimes, are illustrated in Figure 3(B,C), respectively.

Photos were recorded by a digital camera (Canon 500D, Japan) mounted on an optical microscope (BX400, Olympus Optical, Japan). The size distribution of microsphere was analyzed using ImageJ software (available at http://rsb.info.nih.gov/ij/). The average diameter, D_m, and size distribution of the microsphere along with coefficient of variance (C.V., defined as the standard deviation in the measured diameter divided by the average diameter) were calculated from measured values of at least 50 prepared microspheres. The C.V. value, defined as eq. (1), is used to characterize the size distribution of the synthesized microspheres. Where d_i is the diameter of the ith microsphere, d is the volume-mean diameter, and N is the total number of measured microspheres.

$$\text{C.V.} = \frac{\left(\sum (d_i - \overline{d})^2 / N\right)^{0.5}}{\overline{d}} \quad (1)$$

During the operation when a blockage was encountered the following procedure was performed to remove the materials in the microchannels: the device was quickly disassembled., the microchannels and the orifice were washed by a water jet, the microchannels were cleaned by a micrometric metal wire, and finally the microfluidic device's layers were immersed in water at an ultrasonic bath for at least 15 min for cleaning.

RESULTS AND DISCUSSION

Initially, a pure oil phase was used as continuous phase during the synthesis process, but it was impossible to generate stable and separated microdroplets. In the absence of surfactant in the continuous phase, a semi-continuous dispersed phase stream was formed within the oil phase which introduces unstable microdroplet formation and coagulation of *in situ* polymerized microparticles. Therefore, a nonionic surfactant (Palmitic acid) was added to the oil phase at 3% (w/v) to reduce the surface tension between both the phases to facilitate stable microdroplet formation in emulsion and to prevent subsequent coalescence prior to the *in situ* polymerization and post curing. According to the results of optical data analysis, it was confirmed that by utilization of surfactant, the droplets moved in an ordered way along the microfluidic channel without coalescence and did not stick together in the post curing tank. At the further runs even by adequate surfactant, tail-shaped microparticles were formed. It was found that the formation of the tail-shaped microparticles was due to the position of the UV exposure near to the cross junction. In this condition, the microdroplets were polymerized while they were not released their breakup stress to form spherical microparticles, therefore the tail-shaped

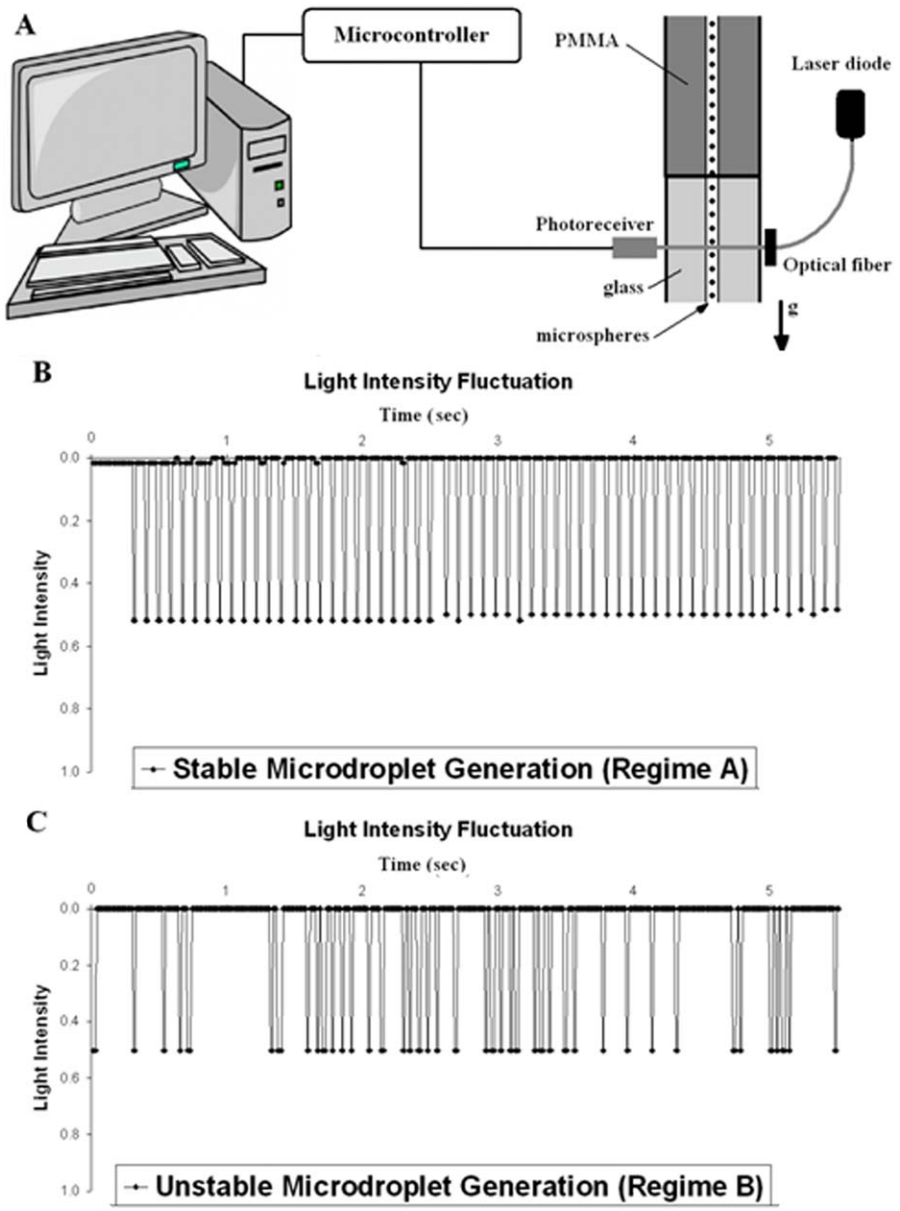

Figure 3. (A) Schematic of optical measurement strategy, the light intensity fluctuation of stable regimes results in monodispersed microspheres synthesis (B) and unstable regimes which result in polydispersed and non-unique microspheres synthesis (C), respectively.

microparticles were formed [Figure 4(K)]. To overcome with this problem, position of the UV exposure window was changed to a farther point from the cross junction. In this way photopolymerization can be performed while the microdroplets were formed fully spherical shape without any shape non-uniformity.

Moreover, semispherical microparticles were obtained in the horizontal platform setup. Considering the noticeable density difference between the dispersed and continuous phases and the low Reynolds numbers streams, migration of microdroplet to the upper layer and the bottom of microfluidic channels can occur. Subsequently, semispherical particles are prepared if the mentioned microdroplets to be cured *in situ*. Based on material properties of the continuous and dispersed phases used in this study (Table I), dispersed phase is denser than the continuous phase; therefore, *in situ* photopolymerization of the generated microdroplets results in semispherical microparticles formation. Conversely, due to unequal UV irradiation to the microdroplets during *in situ* photopolymerization semispherical droplets can be formed. A square aluminum foil was installed at exposure point to reflect UV on the microdroplets for providing a homogeneous photopolymerization condition. Therefore, it was found that the horizontal synthesis process due to higher density of dispersed phase and also no reflector usage resulted in semispherical microparticle formation [Figure 4(L)]. Finally, vertical alignment of microfluidic device by downward flow of fluids was set up to remove the above-mentioned problems during microdroplet formation and *in situ* photopolymerization processes. Also, the semipolymerized microparticles were directed into the horizontal

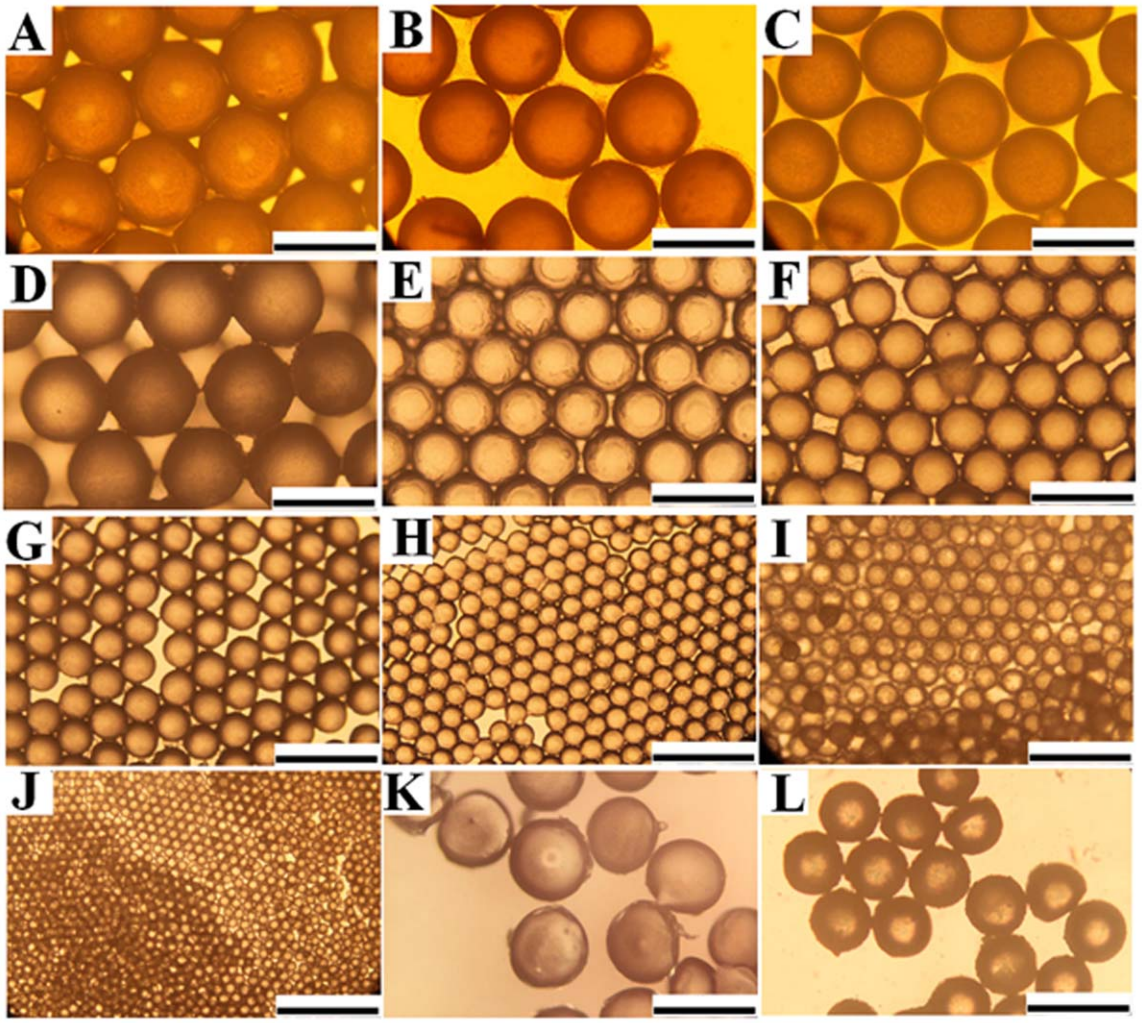

Figure 4. Typical images of the prepared samples at different conditions. Further information by sample code is available in Table II. The scale bar is 200 (μm). [Color figure can be viewed in the online issue, which is available at wileyonlinelibrary.com.]

sedimentation tank for post photopolymerization process. Some typical prepared microsphere samples at the stable regimes are shown in Figure 4.

Flow Rate and Interfacial Effects on Microparticles Formation

When the surfactant is introduced into the continuous phase below 3% (w/v), high interfacial tension between two immiscible fluids leads to generation of irregular microdroplets during *in situ* polymerization and coalescence of microparticles in the post curing sedimentation tank. The concentration of surfactant was optimized (at least ≥3%, w/v) to generate stable microdroplets having spherical shape and a narrow size distribution.

For flow rate ratios (continuous to dispersed) of 2.5–35 and at dispersed phase flow rates within 0.2–1.8 (μL min^{-1}), two kinds of flow patterns are clearly detected after the junction (see Figure 5): stable microdroplets formation (filled and semifilled areas) and unstable flows and non-unique microdroplets formation (unfilled area). Based on the explored flow patterns of the pure HEMA as dispersed phase [Figure 5(A,D)], for $Q_c/Q_d < 5$ and $Q_c/Q_d < 7.5$ and for orifice size of 177 and 269 (μm), it is seen there is a tendency for wetting of the top and/or bottom of the microchannel surfaces and adherence to the orifice resulting in growth of droplets and formation of large and non-uniform microdroplets. Moreover, microchannel blocking occurs when the flow rate of dispersed phase is higher than 1.3 (μL min^{-1}). The stable and monodisperse emulsions can be generated in limited range of $5 < Q_c/Q_d < 25$ and $7.5 < Q_c/Q_d < 30$ when the flow rate of dispersed phase varies from 0.2 to 1.3 (μL min^{-1}) and 0.2 to 1.6 (μL min^{-1}) for orifice size of 177 and 269 (μm), respectively (filled areas as a stable regimes). As the flow rate ratio of continuous to dispersed phase increases, the region of stable microdroplet formation decreases and as a result formation of stable and uniform microdroplets cannot be obtained at the higher flow rate ratios. Moreover, at the higher concentration of the surfactant (5%, w/v) no significant changes in the flow patterns are obtained (i.e., semifilled areas). As a result, it can be concluded that surfactant concentration has very small effect on the process conditions, stable regimes, and microdroplet formation.

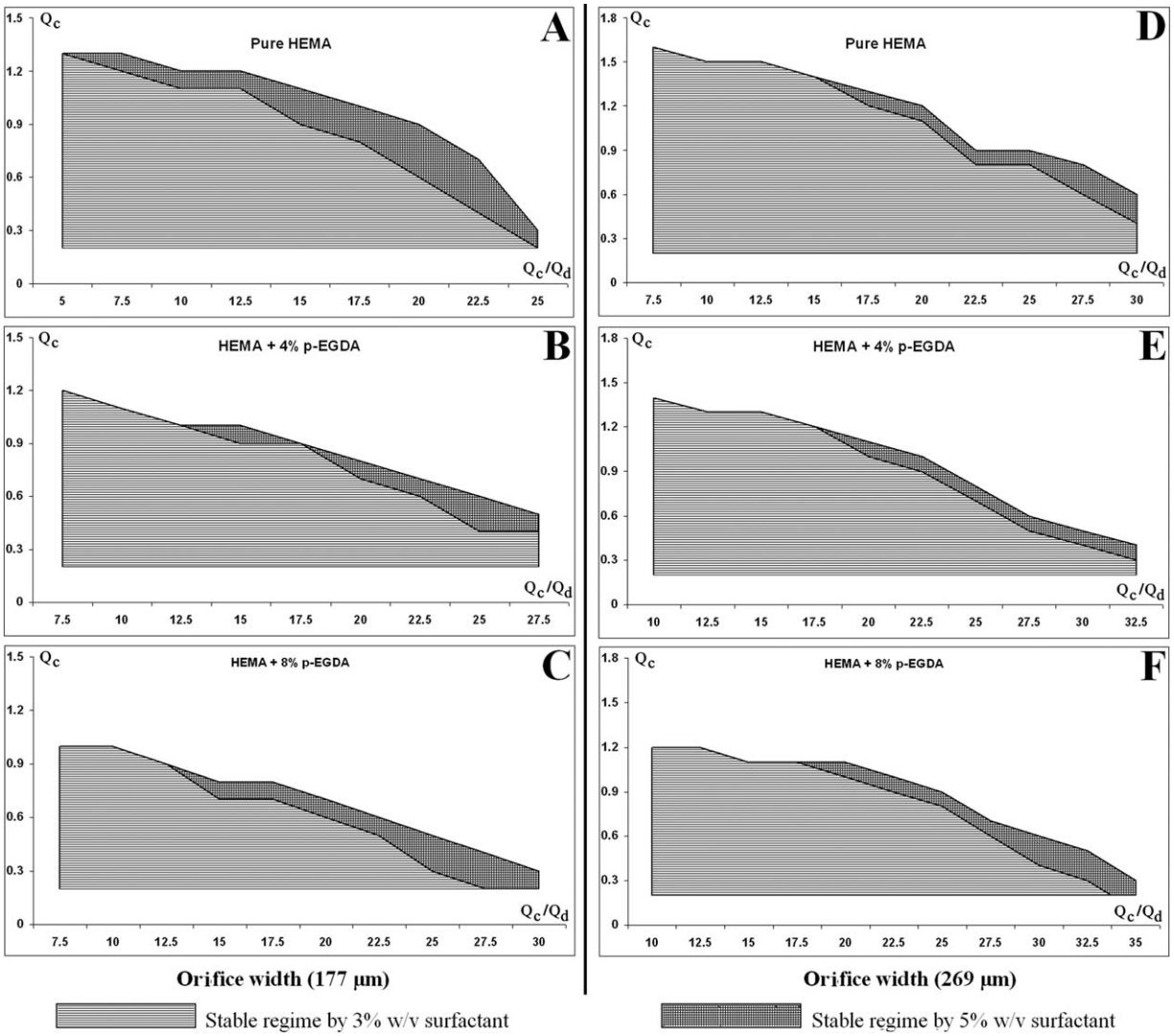

Figure 5. Flow patterns of stable regimes, the left and right hand patterns are for orifice size of 177 and 269 (µm), respectively. Filled and semifilled areas indicate stable regimes when surfactant contents are 3% (w/v) and 5% (w/v), respectively.

The flow patterns of the dispersed phase when 4 and 8 wt % of p-EGDA, as chain extender, were added to the dispersed phase are shown in Figure 5(B,C,E,F). It is seen that by addition of p-EGDA to the dispersed phase, the border of the stable regime shifts to higher flow rate ratios and to lower dispersed flow rates as compared to the neat dispersed phase consisting of HEMA. In this condition initiation of the stable regimes needs at least $Q_c/Q_d > 7.5$ and $Q_c/Q_d > 10$ to form stable microdroplets for orifice size of 177 and 269 (μm), respectively.

At the high flow rate of the continuous phase or very high Q_c/Q_d, a transition from stable to unstable regime or an elongational flow behavior occurs. If the values of C_a or Q_c/Q_d gradually increase at a constant Q_d, a critical capillary number is reached where the dispersed phase begins to elongate and breakup without any order. This is the onset of the transition from the stable microdroplet formation phase (filled and semifilled areas regimes) to unstable microdroplet formation phase (unfilled area

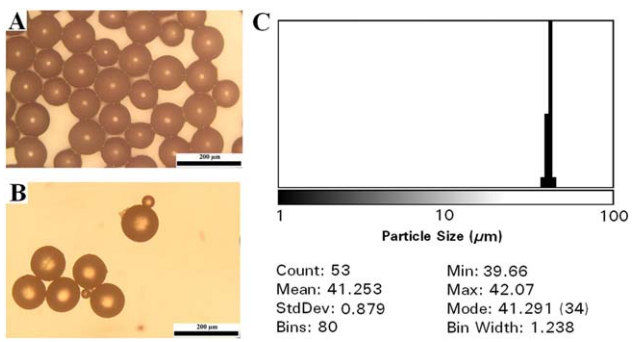

Figure 6. (A) Satellite microspheres prepared by HEMA/8 wt % p-EGDA at $Q_d = 0.8$ (µL min^{-1}) and $Q_c/Q_d = 15$, (B) satellite microspheres prepared by HEMA/8 wt % p-EGDA at $Q_d = 0.5$ (µL min^{-1}) and $Q_c/Q_d = 22.5$, and (C) particle size distribution of sample-I based on ImageJ software. The scale bar is 200 (µm). [Color figure can be viewed in the online issue, which is available at wileyonlinelibrary.com.]

Table II. Mean Diameter, C.V., and Rate of Production of the Prepared Microspheres (Determined Based on Figure 7)

Sample code	HEMA (wt %)	p-EGDA (wt %)	Orifice size (μm)	Q_c/Q_d ratio	Mean diameter (μm)	C.V. (%)	Rate of production (microparticle/s)[a]
A	100	0	269	20	230.15	1.64	1
B	92	8	269	25	198.75	1.21	1.6
C	96	4	269	25	181.4	1.32	2.1
D	92	8	177	7.5	170.17	3.02	2.6
E	96	4	177	12.5	109.37	1.56	9.7
F	92	8	177	17.5	68.06	2.74	40.4
G	96	4	177	17.5	58.53	2.33	63.5
H	100	0	177	17.5	43.12	2.38	158.8
I	92	8	177	22.5	41.25	2.13	181.5
J	100	0	177	22.5	16.27	3.78	2957.8

[a] Based on theoretical calculation (volume of dispersed phase flow rate divided by the volume of microparticle).

regime). Therefore, monodisperse microdroplets cannot be generated beyond the stable regime borders.

Moreover, at the borders of the stable to unstable regimes a transition to a jetting mode occurs.[25] In this condition, the dispersed phase passing through the flow-focusing orifice break off into main population of microdroplets while some of them accompany with small or big satellite microdroplet [Figure 6(A,B)]. The satellites microparticle diameter is found to be larger when synthesis process is done at lower dispersed flow rates and flow rate ratios when moving on the transition line.

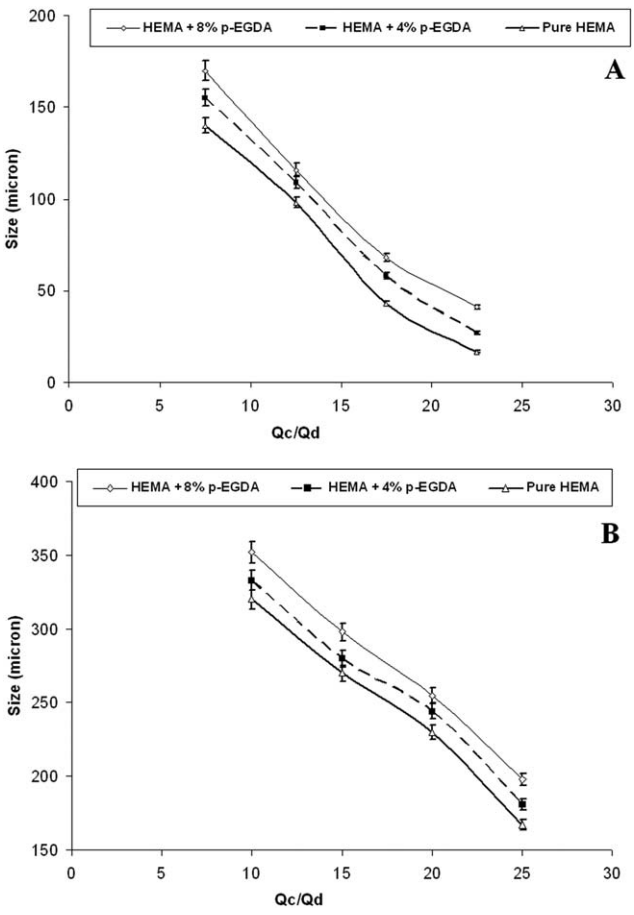

Figure 7. Variation of mean diameters of the prepared microspheres versus the flow rate ratios, (A) orifice size of 177 (μm) and Q_d fixed at 0.4 (μL min^{-1}), (B) orifice size of 269 (μm), and Q_d fixed at 0.4 (μL min^{-1}).

The mean diameters and C.V. of the prepared microspheres as a function of the flow rate ratios at different compositions of the HEMA/p-EGDA were summarized in Table II. Figure 7(A,B) shows the effect of composition of the HEMA/p-EGDA mixture and flow rate ratios on microspheres size at $Q_d = 0.4$ (μL min^{-1}) for orifice dimensions of 177 and 269 (μm), respectively. It is found that at the stable regimes and fixed dispersed phase flow rate, microspheres size decreases by increasing of the flow rate ratios. Moreover, the decreasing trends of the microspheres diameter by flow rate ratios for orifice size of 177 (μm) are more pronounced than that of the orifice with the higher size (269 μm).

Effect of Components on Microparticles Formation

As mentioned in the previous section, wetting phenomenon was detected for $Q_c/Q_d < 5$ (pure HEMA as dispersed phase). Such wetting phenomenon was almost seen for all the cases of $C_{p\text{-}EGDA} = 4$ and 8 wt %. By increasing $C_{p\text{-}EGDA}$ the borders of the stable regimes shifted to the higher flow rate ratios as shown in Figure 5(D–F). In this condition, breakup of the dispersed phase becomes harder when $C_{p\text{-}EGDA}$ increases which might be due to viscosity effect of the dispersed phase. It is obviously due to the fact that the continuous phase cannot effectively surround, push, and break up the dispersed phase after they passed through the inner fluid orifice at low flow rate ratios particularly when viscosity of dispersed phase increases. Therefore, higher flow rate ratios are needed to break up dispersed phased into microdroplets.

For the applied flow rate ratios, it is found that an increase in $C_{p\text{-}EGDA}$ from 0 to 8 wt % results in an increase in the microspheres diameter (Table II). By fixing the flow rates of the dispersed phase and flow rate ratios, the size of microspheres increases linearly with increasing $C_{p\text{-}EGDA}$ from 0 to 8 (wt %). The effect can be attributed to the fact that the increase of $C_{p\text{-}EGDA}$ (wt %) increases dispersed phase viscosity and interfacial tension with respect to the continuous phase (Table I).

After size distribution measurement of the prepared microspheres (at least 50 particles), a coefficient of variance (C.V.) less than 4% is obtained (the results are summarized in Table II). The C.V. is defined as the ratio between the standard deviation of the diameter and the mean diameter. The C.V. of the microspheres increases by increasing of the flow rate ratios. In other words, broader particle size distribution is detected when process is performed at higher flow rate ratios or at higher continuous phase flow rates in the stable regime. A C.V. of less than 5% is the commonly accepted definition of monodispersity. Particle size distribution diagram of a prepared microspheres, HEMA/8 wt % p-EGDA [Figure 4(I)], at the flow rate $Q_d = 0.4$ μL min^{-1} and flow rate ratio of 22.5 are shown in Figure 6(C). The image shows narrow particle size distribution and also C.V. of 2.13% which confirms high monodispersity index.

Based on the findings from this study it can be concluded that dispersed phase viscosity plays a prominent role on microspheres diameter as well as on the flow rate ratios. Thus, the mean diameter of the microspheres can be gently manipulated by controlling flow rate of continuous phase and viscosity of the dispersed phase, ranging from 16 to 340 (μm) in these experiments. In addition, the prepared microspheres in the stable regime of microdroplet formation show high monodispersity (C.V. $< 4\%$) which is acceptable for many biological applications. Moreover by increasing $C_{p\text{-}EGDA}$ (wt %) from 0 to 8%, it is found that lower time is needed to completely solidify the microdroplets to microspheres. This is mainly due to effect of the density distribution of the p-EGDA used as crosslinking agent or chain extender.

CONCLUSION

Many experiments were conducted to document the formation of two-phase W/O dispersions in microchannels fabricated with the flow-focusing configuration based on laser direct writing on PMMA sheets. The applied microfluidic technique was simple but efficient enough to generate p-HEMA based microspheres with high degree of monodispersity. Microspheres were synthesized in vertical alignment due to noticeable differences between densities of dispersed and continuous phases. It was observed that the formation of monodisperse microdroplets, stable regimes, occurs over a wide range of flow rates of dispersed phase and flow rate ratios obviously depending on the continuous phase composition, flow rate ratios, orifice size, and surfactant content of the continuous phase. Using continuous microdroplet formation instable regimes and *in situ* photopolymerization, microspheres were synthesized with sizes from 16 to 340 (μm) and C.V. $< 4\%$ which is fairly acceptable for many biological, drug delivery, and chromatography applications. It was concluded that flow rate ratio plays a more prominent role on microdroplet size formation in both the orifice sizes, 177 and 269 (μm). Addition of p-EGDA to the continuous phase increased microspheres diameters compared to the pure HEMA.

REFERENCES

1. Bagwe, R. P.; Kanicky, J. R.; Palla, B. J.; Patanjali, P. K.; Shah, D. O. *Crit. Rev. Ther. Drug Carrier Syst.* **2001**, *18*, 77.
2. Beneš, M. J.; Horák, D.; Svec, F. *J. Sep. Sci.* **2005**, *28*, 1855.
3. Bouquey, M.; Serra, C.; Berton, N.; Prat, L.; Hadziioannou, G. *Chem. Eng. J.* **2008**, *135*, S93.
4. Champion, J. A.; Katare, Y. K.; Mitragotri, S. *J. Control. Rel.* **2007**, *121*, 3.
5. Chow, A. H. L.; Tong, H. H. Y.; Chattopadhyay, P.; Shekunov, B. Y. *Pharm. Res.* **2007**, *24*, 411.
6. Dendukuri, D. Microfluidic Approaches to the Synthesis of Complex Polymeric Particles (Doctoral Dissertation, Massachusetts Institute of Technology), **2007**.
7. Duncan, A. C.; Boughner, D.; Campbell, G.; Wan, W. K. *Eur. Polym. J.* **2001**, *37*, 1821.
8. Gravesen, P.; Branebjerg, J.; Jensen, O. S. *J. Micromech. Microeng.* **1998**, *3*, 168.
9. Herold, K. E; Rasooly, A. Lab on a Chip Technology: Fabrication and Microfluidics; Horizon Scientific Press: Norwich, UK, **2009**; Vol. *1*.
10. Hung, L. H.; Lee, A. P. *J. Med. Biol.* **2007**, *27*, 1.
11. Li, W.; Nie, Z. H.; Zhang, H.; Paquet, C.; Seo, M.; Garstecki, P.; Kumacheva, E. *Langmuir* **2007**, *23*, 8010.
12. Ma, H.; Su, Z. Microspheres and Microcapsules in Biotechnology: Design, Preparation and Applications; Pan Stanford Publishing: Singapore, **2013**.
13. Michael, K.; Evans, A.; Brunnschweiler, A. Microfluidic Technology and Applications; Research Studies Press: Baldock, UK, **2000**.
14. Qu, H.; Gong, F.; Ma, G.; Su, Z. *J. Appl. Polym. Sci.* **2007**, *105*, 1632.
15. Sahil, K.; Akanksha, M.; Premjeet, S.; Bilandi, A.; Kapoor, B. *Int. J. Res. Pharmacy Chem.* **2011**, *4*, 1184.
16. Qadeer, A.; Attinger, D.; Chen, W. *J. Appl. Polym. Sci.* **2011**, *121*, 3093.
17. De Rosa, R. L.; Noni, L. M.; Hendrick, E. S. *J. Appl. Polym. Sci.* **2007**, *105*, 2083.
18. Sajeesh, S.; Chandra, P. Polymeric Nano/Microparticles for Oral Delivery of Proteins and Peptides, in Biomaterials Fabrication and Processing Handbook, Chu, P. K., and Liu, X. (Eds.); CRC Press, Taylor & Francis Group, FL, USA, Chapter 7, **2008**.
19. Shaha, R. K.; Shuma, H. C.; Rowata, A. C.; Lee, D.; Agrestia, J. J.; Utadaa, A. S.; Chua, L. Y.; Kima, J. W.; Nievesa, A. F.; Martineza, C. J.; Weitza, D. A. *Mater. Today* **2008**, *11*, 18.
20. Singh, M. N.; Hemant, K. S. Y.; Ram, M.; Shivakumar, H. G. *Res. Pharm. Sci.* **2010**, *5*, 65.
21. Song, H.; Delai, L.; Ismagilov, R. F. *Angew. Chem. Int. Ed.* **2006**, *13*, 7336.
22. Squires, T. M.; Quake, A. R. *Rev. Modern Phys.* **2005**, *77*, 977.
23. Tabeling, P. *Phys. Fluids* **2010**, *22*, 021302.
24. Takasi, N.; Hatsuzawa, K. *Microfluidics Nanofluidics* **2010**, *9.2*, 427.
25. Wang, J. W.; Wang, J.; Han, J. *J. Small* **2011**, *7*, 1728.
26. Capretto, L.; Mazzitelli, S.; Balestra, C.; Tosi, A.; Nastruzzi, C. *Lab Chip* **2008**, *8*, 617.
27. De Geest, B. G.; Urbanski, J. P.; Thorsen, T.; Demeester, J.; De Smedt, S. C. *Langmuir* **2005**, *21*, 10275.